OPTOELECTRONICS AND ADVANCED MATERIALS – RAPID COMMUNICATIONS Vol. 4, No. 9, September 2010, p. 1310 - 1315

# Nanoparticles and nanoparticle aggregates sizing by DLS and AFM

D. CHICEA
*Physics Dept., University Lucian Blaga of Sibiu, Dr. Ion Ratiu Str. 7-9, Sibiu, 550012, Romania*

Nanofluids are suspensions of nano to micrometer sized particles in liquids. A nontypical Dynamic Light Scattering experiment was conducted for measuring the nanoparticles and the aggregates diameter in aqueous suspension. Atomic Force Microscope (AFM) measurements were also carried on and the results are discussed.

(Received June 29, 2010; accepted September 15, 2010)

*Keywords*: $Fe_3O_4$ nanoparticles Dynamic Light Scattering, Atomic force microscopy

## 1. Introduction

When a small amount of nanoparticles is added to a fluid, the heat transfer properties are considerably enhanced [1]. Such a suspension is currently named a nanofluid; it is a relatively new notion and was first mentioned by Choi in 1995 [2].

Gravity, Brownian force, buoyant and friction force between fluid and the particles lead to a continuous, irregular motion of the nanoparticles in nanofluids. The irregular nanoparticle motion in the fluid is the cause the remarkable enhancement of heat transfer properties of the nanofluids [3-6]. The irregular motion directly depends of the particle dimension therefore the particle size distribution dictates the rheological properties of the nanofluid.

The living cells have dimensions of the order of microns and parts of the order of tens to hundreds of nanometers. Some proteins are even smaller, having dimensions around 5 nanometers. With this in mind, it was easy to imagine that nanoparticle structured materials can be used in many ways to investigate, to modify living cells or to deliver certain substances or drugs to them without perturbing much the cells. Thus many practical applications were developed in the last years and are nicely presented in [4] and in many other review papers, like [7]. Some of the possible applications can be: drugs and gene delivery [8], biodetection of pathogens [9] and proteins [10], investigation of DNA structure [11], tissue engineering [12], tumour destruction using hyperthermia [13], Magnetic Resonance Imaging contrast enhancement [14], to mention just a few of them.

The nanoparticles usually form the core of nano-biomaterial; it can be used as a convenient surface for a molecular assembly, and may be composed of inorganic or polymeric materials. The typical shape is spherical but other shapes as cylindrical and plate-like are possible. The size and size distribution is crucial if penetration through a cellular membrane is intended. The size and size distribution are extremely important when quantum-sized effects are used to control material properties, as well. A tight control of the average particle size and a narrow distribution of sizes allow creating fluorescent probes that emit narrow light in a very wide range of wavelengths [7].

Once a nanoparticle sample is prepared, it is characterized; the average particle size and size distribution are some of the mandatory physical properties to be determined. The Transmission Electron Microscopy (TEM) is currently used in characterizing nanoparticles and nanometer to micrometer sized clusters. While it offers the best resolution, the sample requires specific preparation to be shaped as a very thin film and finally is placed in vacuum and becomes target for the electron beam. The technique is expensive and time consuming.

A convenient approach is to use optical methods involving a coherent light scattering experiment. The target is the suspension, the far field is recorded and the statistical analysis of the speckle image is performed. The speckled image appears as a result of the interference of the wavelets scattered by the scattering centers (SC hereafter), each wavelet having a different phase and amplitude in each location of the interference field. The image changes in time as a consequence of the scattering centers complex movement of sedimentation and Brownian motion giving the aspect of "boiling speckles" [15], [16]. In papers like [17] an optical set-up is used to measure the correlation function in the near field, and reveals the near-field speckle dependence on the particles size. The work reported in [18], [19] uses a transmission optical set-up to measure the far field parameters like contrast and speckle size and reveals that speckle size and contrast are related with the average particle diameter. Reference [20] revealed a strong variation of the average speckle size and contrast with the concentration of the scattering centers, but the work described here deals with samples that can have both different nanoparticle concentration and size, therefore the speckle analysis technique is not the best suited for particle sizing.

A convenient alternative to these techniques and others not mentioned in this introductory part is based on the fact that the nanoparticles have a continuous, irregular motion in nanofluids, which is the effect of several factors such as Brownian force, buoyant force, friction force between fluid and the particles and gravity, which becomes significant for micron sized particles but can be

neglected for nanometer sized particles [21], [22], [23]. The method is called Dynamic Light Scattering (DLS) or Photon Correlation Spectroscopy (PCS) and the physical principles of the method are explained in [15 -17] and other papers following them. The DLS technique was used in the work reported here to assess the average nanoparticle size and is described in the dedicated section of this paper.

Another optical alternative to measure the average nanoparticle size in suspension is the modified version of the Static Light Scattering (SLS) experiment. The light scattering anisotropy coefficient *g* strongly depends of the scattering center diameter. A functional dependence of the g parameter with the nanoparticle diameter can be derived using Mie calculations. Once the g parameter is measured using a least square fit, the average diameter can be derived using the functional dependence calculated for that particular type of nanoparticles, as described in [24].

An alternative technique that can be used to assess the nanoparticle size is the Atomic Force Microscopy (AFM). One of the papers that reports using AFM for nanoparticle sizing is [25]. A comparison of the TEM with the AFM results is presented in [26]. The results in [25] reveal that the AFM measured nanoparticle diameter appears to be reduced with 20% and the standard deviation appears to be increased with 15%. The differences in the diameter and in the standard deviation findings were associated with the AFM tip and the nanoparticle concentration on the substrate. The AFM technique and the results using it are presented in the dedicated section of this paper.

The following section describes the DLS procedure used for assessing the average nanoparticle size.

## 2. Nanoparticle sizing by DLS

The procedure we used to prepare the aqueous nanofluid is a typical coprecipitation. The reagents used were: $FeCl_2 \cdot 4H_2O$, $FeCl_3 \cdot 6H2O$, ammonium hydroxide ($NH_3$[aq]), citric acid ($C_6H_8O_7$), all produced by Merck, Darmstadt. Overall the chemical reaction was:

$$2FeCl_3 + FeCl_2 + 8NH_3 + 4H_2O \rightarrow Fe_3O_4 + 8NH_4Cl \quad (1)$$

The nanofluid was stabilised by coating the nanoparticles with citric acid. The preparation procedure is presented in detail in [27]. In preparing the sample used in the work a stronger stirring was used though, with a mechanical stirrer at 5 rot/second and the result was a smaller average nanoparticle diameter, as it is presented further on.

The Dynamic Light Scattering (DLS) is a technique currently used for measuring particle size over a size range from nanometers to microns. The light scattered by a suspension presents fluctuations [15], [16]. By placing a detector at a certain angle and recording the scattered light intensity a time series is recorded. The width of the autocorrelation function of the time series is proportional to the diffusion coefficient, which, on it's turn, depends of the particle diameter [28], [29]. This leads to a fast procedure for measuring the particle diameter.

The early experimental works [30], [31] and the later theoretical treatises [32 - 34] proved the assumption that the powerspectrum of the intensity of the light scattered by particles in suspension can be linked to the probability density function (hereafter PDF). This link between the PDF and the powerspectrum is a consequence of the translation of the relative motion of the scattering particles into phase differences of the scattered light. Thus spatial correlations are translated into phase correlations. As a consequence of the Wiener-Khintchine-Theorem, the powerspectrum is related to the autocorrelation of a process. The phasecorrelations lead to fluctuations in the intensity of the scattered light recorded using a detector and a data acquisition system, in a typical experimental setup as presented in Fig. 1.

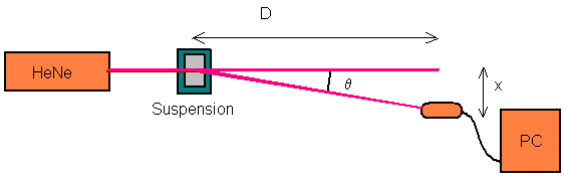


*Fig. 1. A typical DLS experimental setup.*

By subtracting the average intensity from the recorded time series and calculating the square of the intensity we obtain the power time series. The Fourier transform of the power time series is the power spectrum. We can compare the spectrum calculated from the experimental data with the theoretically expected spectrum, namely the functional form of the Lorentzian line S(f), described by equation (3).

$$S(f) = a_0 \cdot \frac{a_1}{(2\pi f) + a^2_1} \quad (2)$$

The Lorentzian line S(f) has two free parameters $a_0$ and $a_1$ and is fit to the powerspectrum using a non-linear minimization procedure to minimize the distance between the data-set and the line. We notice that $a_0$ enters linearly, thus only performing a scaling of the function in the range, which translates into a shift in the logarithmic representation. The $a_1$ parameter enters nonlinearly into the function. Its effect in the loglog scaled plot can approximately be described as a shift along the frequency axis. The possibility to fit the whole function is advantageous compared to the alternative method described in [16], [30], [31], where the $f_{1/2}$ (the frequency where half-maximal-height is reached) was measured, since it takes more data points into account, thus increasing the quality of the fit.

Once the fit is completed and the parameters are found, the diameter of the SCs can be assessed as the double of the radius R. The radius can be derived as a function of the fitted parameter $a_1$ and other known quantities using (3):

$$R = \frac{2k_B TK^2}{6\pi\eta a_1} \quad (3)$$

where

$$K = \frac{4\pi n}{\lambda} \cdot \sin\left(\frac{\theta}{2}\right) \tag{4}$$

In (3) $k_B$ is Boltzman's constant, T is the absolute temperature of the sample, η is the dynamic viscosity of the solvent. In (4) θ is the scattering angle, n is the refractive index of the scattering particles and λ is the wavelength of the laser radiation in vacuum.

The experimental setup and other details are presented in [35]. The wavelength was 633 nm, the light source was a He-Ne laser and the power was 2 mW. The DLS experiment was carried on at 20 $^oC$. The cuvette-detector distance D was 0.59 m and x was 0.05 m making the scattering angle θ equal to 4$^o$ 50' 38.4''. This is not typical for DLS where a bigger angle is chosen, usually 90$^o$. The reason for choosing such a small angle is to shift the rollover point in the Lorentzian line towards smaller $a_1$ values, hence smaller frequencies, where the noise is considerably smaller. These values of the experimental parameters are slightly different from the values used in [35]. The angle is bigger than the angle used in [35], shifting the rollover point towards bigger frequencies. Moreover, the data acquisition rate was 8000 per second, considerably bigger, thus increasing the number of data points to fit he Lorentzian line S(f) (2) to, making the fit more precise.

First the concentrated nanoparticle suspension was diluted in 25% citric acid, in order to prevent aggregation and a DLS time series was recorded. As pointed out in [24] and [35] the aggregation process in diluted aqueous solutions is very fast, therefore an alternative solvent must be used for accurate DLS sizing. The time series was analyzed using the procedure described above. The diameter was found to be 9 nm.

Later on a diluted aqueous suspension was prepared in the cuvette and after 10 seconds a time series was recorded using the experimental setup described above and the parameters previously mentioned. The data processing procedure was used. The PSD (blue line) and the fitted Lorentzian line for the time series recorded on sample l m9-3 are presented in Fig. 2.

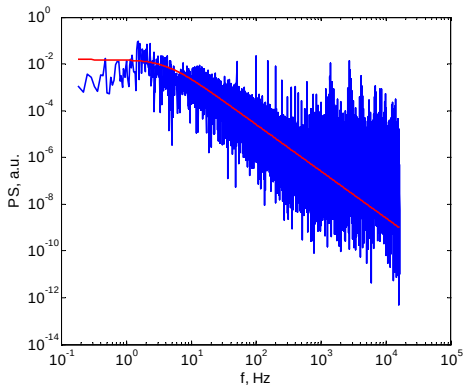


*Fig. 2. The PSD (scattered line) and the fitted Lorentzian line (smooth) for the time series recorded on sample lm9-3 diluted in citric acid.*

The parameters of the Lorentzian line found from the fit are: $a_0$=0.127 and $a_1$=8.2. Using (3) and (4) we found that the SCs have an average diameter of 167 nm. The PSD (blue line) and the fitted Lorentzian line for the time series recorded 10 seconds after dilution initiation is presented in Fig. 2. The aggregation process continues and as pointed out in [24] and [35] after one minute it can be considered that aggregates formation was completed.

## 3. AFM measurements

The atomic force microscope (AFM) is a scanning probe microscope. The AFM uses a flexible cantilever as a type of spring to measure the force between the tip and the sample. The basic idea of an AFM is that the local attractive or repulsive force between the tip and the sample is converted into a deflection of the cantilever. The cantilever is attached to a rigid substrate that can be held fixed, and depending whether the interaction at the tip is attractive or repulsive, the cantilever will deflect towards or away from the surface [36].

The cantilever deflection is converted into an electrical signal to produce the images. The detection system uses a laser beam that is reflected from the back of the cantilever onto a detector. The optical lever principle is used. This states that a small change in the bending angle of the cantilever is converted to a precisely measurable deflection in the position of the reflected spot. By scanning the sample line by line and using a calibration file for each mode of operation and cantilever type a topography image of the surface is reconstructed by the software that drives the scanning process.

The AFM that was used in the work reported here is an Agilent 5500 type. The scanning mode was ACAFM. A soft tip, having the spring constant equal to 5 N/m was used at low force amplitude. As the nanoparticles or nanoparticle aggregates undergo a Brownian motion in suspension, scanning in liquid can not be used for nanoparticle sizing, also the microscope can be used to scan in liquid.

Sample preparation is crucial in order to get useful AFM images. The samples must be thin enough to have a single layer of the objects that are studied, whether they are micron sized cells or nanometer sized particles. The second condition that a sample for AFM imaging must fulfill is that the objects, nanoparticles or aggregates in this case, must adhere well on the surface, otherwise they will be removed by the tip of the cantilever during the scanning process.

First, a drop of nanofluid was deposited on a freshly cleaved mica substrate and stretched with a microscope slide edge to form a very thin layer. The thin layer was left for 3 hours to evaporate. The sample was attached to the AFM plate and for the beginning a large area (5 μm × 5 μm) surface scan was carried on. The 3D rendering type of the surface topography is presented in Fig. 3.

Fig. 3 reveals that during solvent evaporation islands of nanoparticles appeared on the substrate surface. The resolution used in this first scan is not good enough to

image nanoparticles on a surface, therefore several scans were carried on selecting a flat area on the surface where there appears to be no island. Finally, a big resolution scan was achieved and the topography is presented in Fig. 4. The scanned area is 0.5 µm × 0.5 µm.

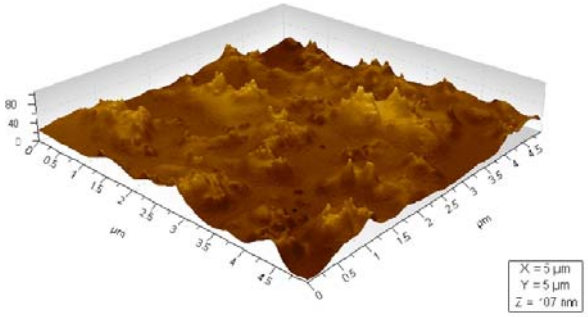


*Fig. 3. The topography of the evaporated nanofluid deposited on a freshly cleaved mica surface. Z axis is in nm.*

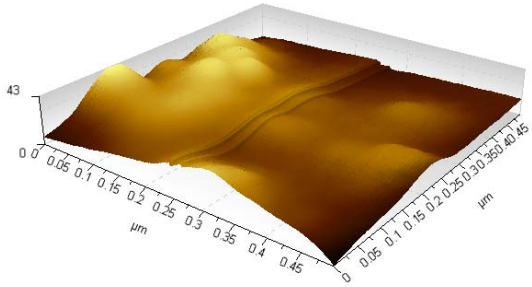

*Fig. 4. A small area on the surface. Z axis is in nm.*

Examining Fig. 4 we notice that the left part is two atomic layers above the right part of the sample, and this is the result of cleaving the mica substrate, which was done right before depositing the sample in order to obtain a clean surface.

We notice in the left upper corner several closed nanoparticles on the surface and other spread across the scanned area. 3D topography images are not the best way to assess nanopartticles dimension, but profiles extracted from the images can produce accurate information. Fig. 5 presents the profile extracted over the three aligned nanoparticles in the left upper corner and Fig. 6 is a profile parallel to the lines that separate the atomic layers of the substrate.

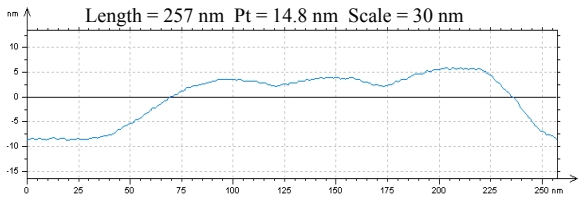


*Fig. 5. The profile extracted over the three aligned nanoparticles in the left upper corner.*

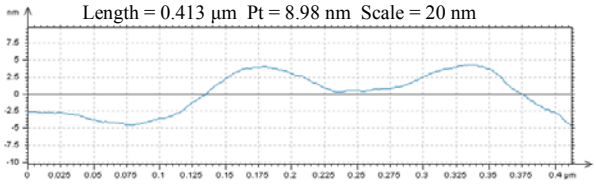


*Fig. 6. A profile parallel to the lines that separate the atomic layers of the substrate.*

The difference between the top and the base line values of the Z axes indicated the dimension of the nanoparticle. Examining the profiles in Fig. 4 and 5 we notice that the size of the nanoparticles is around 9 nm, which is consistent with the DLS nanoparticle sizing experiment results presented in the previous section.

Later on 10 µl of the diluted nanofluid that was diluted in water for the DLS cluster sizing experiment were deposited on a microscope slide. As the dimension of the clusters is considerably bigger, a microscope slide could be used as a substrate. The drop was stretched on the microscope slide using the edge of another clean slide. The thin layer was allowed for three hours to evaporate and than was attached to the plate of the AFM microscope.

A big area (50 µm × 50 µm) surface scan was carried on and the topography of the surface is presented in Fig. 7. We notice that on the Z axis the objects on the surface measure hundreds of nanopameters.

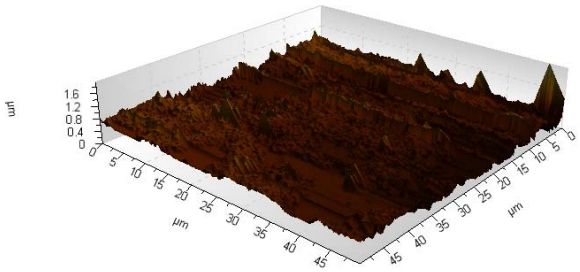

*Fig. 7. Clusters on a microscope slide surface, on a 50 µm x 50 µm area scan.*

In order to assess more precisely the dimension of the objects on the surface several profiles were extracted. Two of them are presented in Fig. 8 and 9.

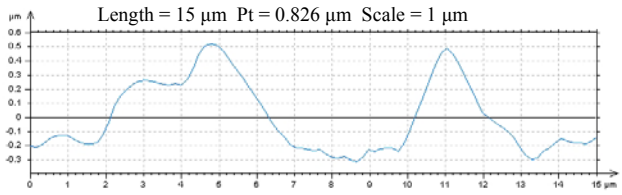


*Fig. 8. A profile on the glass substrate.*

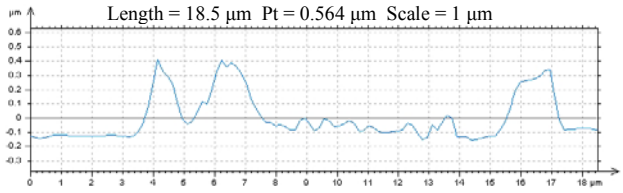


*Fig. 9. Another profile on the glass substrate.*

We notice that the difference between the base line and the top of the cluster in the profile line is in the range of 500 – 800 nm. This result is consistent with the cluster dimension found by DLS.

## 4. Discussions

The two methods used in assessing the nanoparticle dimension, the Dynamic Light Scattering and the Atomic Force Microscopy are essentially different.

In the DLS technique the width of the autocorrelation function of the time series is proportional to the diffusion coefficient, which, on it's turn, depends of the particle diameter [28], [29]. The modified version used in this work uses the power spectrum density, which has a Lorentzian variation with the frequency and the parameters of the curve depend of the diffusion coefficient, which on its turn depends of the particle diameter. Consequently this diameter is not the physical diameter, but the hydrodynamic diameter.

The AFM technique uses an image reconstruction from successive lines acquired during a scan of the surface. A profile can be extracted form the topography of the surface and the particle dimension can be assessed from the profile.

Special care must be taken, as the cantilever tip has a finite dimension, which is not fully controlled by the technology used in manufacturing them. Moreover, the cantilever is a consumable in the AFM technique, as the tip wears out during scanning, by becoming less sharp, therefore having a bigger tip radius. Even the sharp new tips have a tip diameter around 40 nm and are used to scan details on the order of 10 nm. Fig. 10 presents the tip in two different positions during scanning over a nanoparticle.

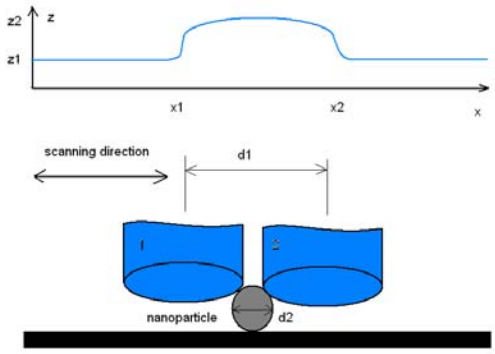


*Fig. 10. The cantilever tip position during scanning over a nanoparticle, when meeting it (1) and when leaving it (2) and the profile.*

The position 1 represents the moment when the tip meets the nanoparticle and 2 when the tip leaves the nanoparticle, when the tip moves from left to right. Above the drawing of the catilever tip the consequent z profile resulting in the scanning process is placed. We notice that the horizontal nanoparticle dimension d1=x2-x1 is much bigger than the actual d2 horizontal dimension of the nanoparticle, while the vertical dimension h=z2-z1 of the nanoparticle matches well the actual vertical dimension of the nanoparticle, if the calibration is correct [37]. With this in mind, when measuring nanoparticles using AFM the horizontal dimension resulting from the topography image or profiles should be avoided but the vertical dimension should be used in assessing the nanoparticle size.

The AFM produces the physical diameter of the nanoparticles on a substrate, not the hydrodynamic diameter as the DLS, therefore the differences that occur in the assessed diameters are natural.

The sample preparation procedure for AFM measuring requires precautions and attention. Nevertheless, it is way faster, easier and less delicate that the sample preparation procedure for TEM imaging.

## 5. Conclusions

In this work two experimental procedures that can be used to assess nanoparticle and nanoparticle aggregates diameter are described and used. The DLS provides an average hydrodynamic diameter of the bigger scattering centers, as presented in [24] and [35] and the diameter is slightly different from the physical diameter. The modified DLS technique presented in [35] can be used to monitor the aggregates formation dynamics.

The AFM technique is more time consuming, as it requires a thin layer deposition on a plane, even atomic layer plane substrate. Moreover the scanning process is time consuming, depending on the desired resolution. It provides the physical diameter of the particle deposited on the substrate. By extracting the dimension of a set pf particles the size distribution can be derived.

The work presented in this article was carried on to compare the two methods. The results were found to be comparable, considering the aspects previously mentioned, therefore we can conclude that the AFM method is a complementary method to the classical DLS. Moreover, the AFM can be used to investigate the small "tale" of the size distribution, while the DLS is significantly less sensitive for smaller sized nanoparticles if the particles have a wider size distribution.

**Acknowledgements**

I am especially indebted to Dr. Gerald Kada of AGILENT for fruitful discussions and training.

## References

[1] P. Vadasz, J. Heat Transfer. **128**, 465 (2006).
[2] U. S. Choi, ASME Fed. **231**, 99 (1995).
[3] S. P. Jang, S. U. S. Choi, Appl. Phys. Lett. **84**,

4316 (2004).
[4] W. Evans, J. Fish, P. Keblinski, Appl. Phys. Lett. **88**, 093116 (2006).
[5] Y. M. Xuan, W. Roetzel, Int. J. Heat Mass Transfer. **43**, 3701 (2000).
[6] R. Prasher, P. Brattacharya, P. E. Phelan, Phys. Rev. Lett. 94, 025901 (2005).
[7] O. V. Salata, Journal of Nanobiotechnology, 2:3, (2004), doi:10.1186/1477-3155-2-3.
[8] D. Panatarotto, C. D. Prtidos, J. Hoebeke, F. Brown, E. Kramer, J. P. Briand, S. Muller, M. Prato, A. Bianco, Chemistry & Biology **10**, 961 (2003).
[9] R. L. Edelstein, C. R. Tamanaha, P. E. Sheehan, M. M. Miller, D. R. Baselt, L. T. Whitman, R. J. Colton, Biosensors Bioelectron, **14**, 805 (2000).
[10] J. M. Nam, C. C. Thaxton, C. A. Mirkin, Science **301**, 1884 (2003).
[11] R. Mahtab, J. P. Rogers, C. J. Murphy, J. Am. Chem. Soc. **117**, 9099 (1995).
[12] J. Ma, H. Wong, L. B. Kong, K. W. Peng, Nanotechnology **14**, 619 (2003).
[13] J. Yoshida, T. Kobayashi, J Magn Magn Mater **194**, 176 (1999).
[14] R. S. Molday, D. MacKenzie, J Immunol Methods **52**, 353 (1982).
[15] J. W. Goodman, Laser speckle and related phenomena, Vol. 9 in series Topics in Applied Physics, J. C. Dainty, Ed., Springer-Verlag, Berlin, Heidelberg, New York, Tokyo, (1984).
[16] J. David Briers, Physiol. Meas. 22 R35 (2001).
[17] M. Giglio, M. Carpineti, A. Vailati, D. Brogioli, Appl. Opt. **40**, 4036 (2001).
[18] Y. Piederrière, J. Cariou, Y. Guern, B. Le Jeune, G. Le Brun, J. Lotrian, Optics Express **12**, 176 (2004).
[19] Y. Piederriere, J. Le Meur, J. Cariou, J. F. Abgrall, M. T. Blouch, Optics Express **12**, 4596, (2004).
[20] D. Chicea, European Physical Journal Applied Physics **40**, 305 (2007) DOI: 10.1051/epjap:2007163.
[21] Z. Xiao, C. Cai, X. Deng, Chem. Commun. 1442 (2001), DOI: 10.1039/b104306b.
[22] S. B. Clendenning, S. F. Bidoz, A. Pietrangelo, G. Yang, S. Han, P. M. Brodersen, C. M. Yip, Z Lu, G. A. Ozin, I. Manners, J. Mater. Chem. **14**, 1686 (2004).
[23] D. Chicea, Applied Optics, **47**(10), 1434 (2008).
[24] D. Chicea, J. Optoelectron. Adv. Mater. **12**(1), 152 (2010).
[25] F. Zhang, S. W. Chan, J. E. Spanier, E. Apak, Q. Jin, R. D. Robinson, I. P. Herman, Appl. Phys. Lett. **80**, 27 (2002); doi:10.1063/1.1430502.
[26] L. M. Lacava, B. M. Lacava, R. B. Azevedo, Z. G. M. Lacava, N. Buske, A. L. Tronconi, P. C. Morais, Journal of Magnetism and Magnetic Materials, **225**(1-2), 79 (2001).
[27] D. Chicea, C. M. Goncea, Optoelectron. Adv. Mater. – Rapid Comm. **3**(3), 185 (2009).
[28] W. Tscharnuter, in Encyclopedia of Analytical Chemistry, R. A. Meyers (ed), John Wiley & Sons Ltd, 5469 (2000).
[29] B. B. Weiner, Chapt. 5 in Liquid-and Surface-Borne Particle Measurement Handbook, J. Z. Knapp, T. A. Barber and A. Liebermann (ed), Marcel Dekker Inc. NY, (1996).
[30] N. A. Clark, Lunacek JH, Benedek GB, American Journal of Physics, **38**(5), 575 (1970).
[31] S. B. Dubin, Lunacek JH, Benedek GB, PNAS, **57**(5), 1164 (1967).
[32] Berne and Pecora, Dynamic Light scattering, John Wiley, 1975.
[33] J. W. Goodman, Statistical Optics, Wiley Classics Library Edition, 2000.
[34] E. Hecht, Optics, Addison-Wesley, New York, 2001.
[35] D. Chicea, Optoelectron. Adv. Mater. – Rapid Comm. **3**(12), 1299 (2010).
[36] http://www.jpk.com/general-scanning-probe-microscopy.431.html
[37] Dr. Gerald Kada, AGILENT, private communication.

*Corresponding author: dan.chicea@ulbsibiu.ro